Polymorphic Behavior of Syndiotactic Polystyrene-Based Graft Copolymers with Polystyrene and Polyisoprene Side Chains

Kazunobu Senoo,*,†,‡ Kiyoshi Endo,‡ Masatoshi Tosaka,† Syozo Murakami,† and Shinzo Kohjiya†

Laboratory of Polymer Condensed States, Institute for Chemical Research, Kyoto University, Uji, Kyoto-fu 611-0011, Japan, and Department of Applied Chemistry, Faculty of Engineering, Osaka City University, Sugimoto, Sumiyoshi-ku, Osaka 558-8585, Japan

Received July 17, 2000; Revised Manuscript Received December 18, 2000

ABSTRACT: Polymorphic behaviors of two types of syndiotactic graft copolymers (syndiotactic polystyrene (SPS) having side chains of polyisoprene (PIP), namely SPS-*graft*-PIP, and SPS having side chains of atactic polystyrene (APS), namely SPS-*graft*-APS) were investigated. Though the as-prepared samples of the both types were in the δ form as well as the homopolymer, they showed different polymorphic behaviors. Furthermore, while SPS-*graft*-PIP and SPS-*graft*-APS with the lower contents of the APS side chains could crystallize from the melt, SPS-*graft*-APS with the higher contents of APS was in an amorphous state. The effect of the graft chains on crystallinity was discussed in terms of the friction force for reptation and the cohesive power; the former may be increased by the side chains in both types of the graft copolymers, while the latter may be enhanced only in the case of SPS-*graft*-PIP, compensating the increment of the friction force.

Introduction

Since the first synthesis of syndiotactic polystyrene (SPS) by Ishihara et al.[1] in 1986, crystallization of this polymer has been of interest because of its complicated polymorphism[2,3] as well as the relatively fast rate of crystallization. The existence of four major crystalline forms, α, β, γ, and δ, along with two types of mesomorphic forms (according to the nomenclature by Italian researchers[3,4]) has been reported so far. The trigonal α and the orthorhombic β forms are characterized by trans planar conformation of the molecular chains. Both of these two forms are divided further into two modifications having different structure order (α' and α'',[3,5,6] β' and β''[7−13]). On the other hand, the γ and δ forms are characterized by the TTGG conformation of the molecular chains. The δ form is termed for clathrate structures including solvent molecules.[14,15] On heating a sample in the δ form, it transforms into the γ form by removing the solvent molecules and by rearranging the chain packing.[15] The "planar" and "helical" mesomorphic forms are not crystalline forms but contain a noticeable amount of trans planar and helical (TTGG conformation) chains, respectively.[4]

In 1998, we reported the synthesis of a graft copolymer composed of SPS main chain and polyisoprene (PIP) side chains by combining the metallocene polymerization technique with the macromonomer method.[16] We have hitherto successfully synthesized two types of syndiotactic graft copolymers by using cyclopentadienyl titanium trichloride ($CpTiCl_3$) in combination with methylaluminoxane (MAO) catalyst. One type is SPS having side chains of PIP, namely SPS-*graft*-PIP.[16,17] The other is SPS having side chains of atactic polystyrene (APS), namely SPS-*graft*-APS.[18] Though the monomer reactivity ratio in the synthesis of these graft copolymers is not fully established,[19] it is supposed that the incorporation of the macromonomers was random because the number of branched chains per molecule is small. It is unclear how the introduction of the long side chains affects the crystallization of the SPS main chain. While the depression in crystallinity by the introduction of chain branching is well-known in the case of polyethylene,[20] more complicated crystallization behaviors are expected for these graft copolymers in terms of polymorphism and of the miscibility between the main chain and side chain segments. APS homopolymer is reported to be miscible to SPS,[21−23] while PIP is immiscible to SPS. These different properties of the side chains should give different effects on the crystallization of the main chain of SPS.

There are some reports about the influence of heterogeneity on polymorphic behavior of SPS.[23−28] For example, Manfredi et al.[24] studied random copolymers of SPS with *p*-methylstyrene (*p*-MS) comonomeric units. The copolymer samples were crystallized from the melt, and their polymorphic behaviors were discussed. The influence of blending SPS with miscible amorphous polymers on the polymorphic behavior was reported by Woo et al. and Guerra et al.[27,28] While APS did not affect the polymorphism of SPS, blending with poly(2,6-dimethyl-1,4-diphenylene oxide) (PPO) changed the polymorphic behavior. For example, when a thermal condition that should give the α form for pure SPS is adopted to the blend sample with a large amount of PPO, the β form rather than the α form was obtained.

In this paper, we examine the thermal behavior of the graft copolymers in view of the crystallinity and the polymorphism, along with SPS homopolymer.[29]

Experimental Section

Synthesis of the Samples. The synthesis of the graft copolymers and the SPS homopolymer used in this study has been reported elsewhere.[16−18] Styrene-terminated polyisoprene macromonomer (SIPM) and styrene-terminated polystyrene macromonomer (SSTM) were synthesized by the reaction of

† Kyoto University.
‡ Osaka City University.
* To whom correspondence should be addressed. Tel +81-774-38-3064; fax +81-774-38-3067; e-mail senoo@scl.kyoto-u.ac.jp.

10.1021/ma001238a CCC: $20.00
Published on Web 01/26/2001

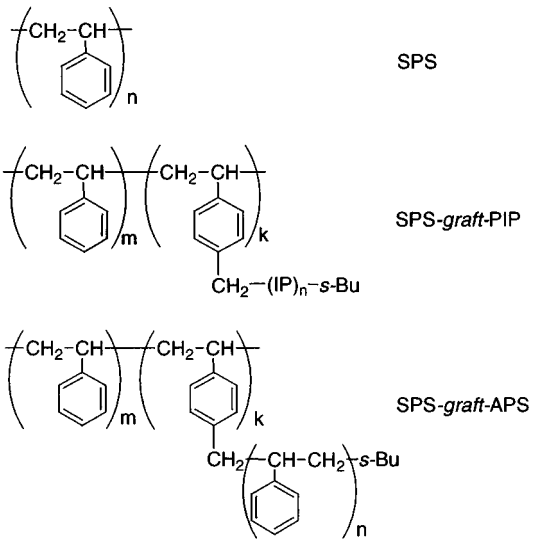

Figure 1. Molecular structures of SPS, SPS-*graft*-PIP, and SPS-*graft*-APS.

Table 1. Copolymerization of St and the Macromonomers (MM) with $CpTiCl_3$, MAO Catalyst in Toluene at 50 °C for 3 h[a]

code	MM content[d] (wt %)	$M_n \times 10^{-4}$	M_w/M_n	no. of MM per molecule
SPS	0	3.90	1.73	0
SPS-*graft*-PIP-9.2[b]	9.2	2.88	1.57	1.4
SPS-*graft*-PIP-19.4[b]	19.4	1.79	1.68	1.8
SPS-*graft*-APS-11.8[c]	11.8	3.10	1.67	3.3
SPS-*graft*-APS-17.3[c]	17.3	3.64	1.77	5.7

[a] [SIPM]; $M_n = 2000$, $M_w/M_n = 1.12$, $f = 0.97$, [SSTM]; $M_n = 1100$, $M_w/M_n = 1.09$, $f = 0.98$. [b] [St] = 2.9 mol/L, [Ti] = 3.1×10^{-4} mol/L, MAO/Ti = 500 (mole ratio). [c] [St] = 2.9 mol/L, [Ti] = 4.7×10^{-4} mol/L, MAO/Ti = 500 (mole ratio). [d] Calculated by the ^{1}H NMR spectrum.

p-chloromethylstyrene with the living polymer of isoprene and styrene, respectively. On the basis of the ^{1}H NMR spectroscopic analysis, the functionalities of the SIPM and the SSTM were estimated to be 0.97−0.98. The SIPM had $M_n = 2.0 \times 10^3$, $M_w/M_n = 1.12$, and a microstructure of *cis*-1,4 (69.9%), *trans*-1,4 (23.1%), and 3,4-units (7.0%). SSTM had $M_n = 1.1 \times 10^3$ and $M_w/M_n = 1.09$. By the copolymerization of styrene and each macromonomer, two types of syndiotactic graft copolymers (Figure 1) were obtained. One is SPS-*graft*-PIP consisting of SPS in the main chain with the side chains of PIP. The other is SPS-*graft*-APS consisting of SPS in the main chain with the side chains of APS. The characteristics of the synthesized samples are listed in Table 1. Because the amounts of the samples were quite limited, only three of the five samples (SPS, SPS-*graft*-PIP-19.4, and SPS-*graft*-APS-17.3) were fully investigated, and the others shall appear in a few parts of this paper.

After the copolymerization in toluene, the solution containing the copolymer was poured into a large amount of methanol with dilute hydrochloric acid. The precipitated copolymer was filtered and washed with methanol and dried and then further washed with methyl ethyl ketone to remove unpolymerized macromonomer and stereoirregular components. The samples were dried under vacuum at 25 °C for 12 h. We denote this sample as "as-prepared" samples in the following part of this paper.

Preparation of Blend Samples. As for blend samples of SPS with APS, those of different origins were used. SPS ($M_w = 1.12 \times 10^6$) was kindly supplied by Idemitsu Petrochemical Co., Ltd. APS ($M_w = 2.8 \times 10^5$) was purchased from Scientific Polymer Products, Inc. Samples containing 0, 21, 50, 78, and 100 wt % of APS were prepared in the similar way as in Guerra et al.[27,28] As is so in Table 1, we indicate the weight percent of the APS component by the number connected to the name of the sample; for example, SPS-*blend*-APS-21 means the blend sample containing 21 wt % of APS. To distinguish from the samples that we synthesized, pure SPS and pure APS of this series are denoted as SPS-*blend*-APS-0 and SPS-*blend*-APS-100, respectively.

Characterization. Most of experiments by differential scanning calorimetry (DSC) were performed by using Seiko S II EXSTAR 6000 thermal analyzer at a heating rate of 10 °C/min in nitrogen atmosphere. The DSC experiments for SPS-*blend*-APS were performed by using Rigaku DSC8230B.

WAXD was carried out using a rotating-anode X-ray generator (Rigaku-Denki, RU-300) operated at 40 kV and 120 mA. Cu Kα radiation monochromatized with a graphite monochromator was shone onto the specimen through a pinhole collimator of 0.5 mm diameter. Each two-dimensional diffraction pattern was recorded onto an imaging plate (IP) and was read out as digital data for a computational process by using an IP system (MAC Science, DIP-220) and our homemade software. In this case, the diffraction pattern was converted to a two-dimensional plate camera, and accordingly, a concentric powder pattern was obtained. The radial intensity distribution was calculated from the concentric pattern. The sample stage of the WAXD instrument was equipped with a specially designed temperature furnace.[30] By blowing thermostated hot air onto the specimen, we can control the specimen temperature uniformly over the whole specimen. According to the former studies[3,4] on SPS by WAXD powder diffractogram using the Cu Kα radiation, the four crystalline forms are characterized as follows: Along with a strong peak at 2θ = ca. 20° observed for all the four crystalline forms, the α form shows a strong peak at $2\theta = 6.7°$ and several weak peaks between $2\theta = 10°$ and 15°. The existence of several weak peaks between $2\theta = 15°$ and 19° indicates the sample is in the α″ modification, and the absence of such peaks indicates the sample is in the α′ modification. On the other hand, the β form shows strong peaks at $2\theta = 6.2°$ and 18.5° along with a very strong peak at $2\theta = 12.3°$; the latter is noted for differentiation from the α form. When there is a peak at $2\theta = 15.7°$ and a shoulder at $2\theta = 11.5°$, the sample is in the β'' modification; the absence of this peak and shoulder indicates that the sample is in the β' modification. The γ form is identified by the strong peak at 2θ = ca. 16° and weak peaks around $2\theta = 10°$. The δ form is characterized by the existence of strong peaks at 2θ = ca. 18° and ca. 23°. The "planar" mesomorphic form is characterized by two broad peaks at $2\theta = 12°$ and 20.5°, while the position of the two peaks in the "helical" mesomorphic form is shifted to $2\theta = 10°$ and 19.5°, respectively.

Atomic force microscopy (AFM) was carried out with a SPM-9500J2 (Shimadzu Inc., Japan) in the dynamic mode, where the cantilever is oscillated close to its resonance. The change of the vertical cantilever oscillation amplitude is detected, which is caused by the interaction of the tip with the surface. Silicon cantilevers (type NCHR-16, NANOSENSORS Dr. Olaf Wolter GmbH, Germany; typical length 125 μm, width 30 μm, thickness 4 μm, spring constant 42 N/m, resonance frequency 330 kHz) were used. The height signal was recorded, and three-dimensional images computed from the height data were displayed. The AFM scanner was placed on an air-spring vibration insulator. Before recording the data, the instrument and the samples were aged more than 1 h by the scanning operation. This aging serves to reduce the specimen drift that is induced thermally.

Results and Discussion

Polymorphic Behavior of As-Prepared Samples on Heating. The DSC charts for the heating scan at 10 °C/min of as-prepared samples are shown in Figure 2. Each sample presented two endothermic peaks in the DSC chart; one is a sharp peak in the 80−100 °C range, and another is a relatively broad peak in the 160−270 °C range. Between these endothermic peaks, the exist-

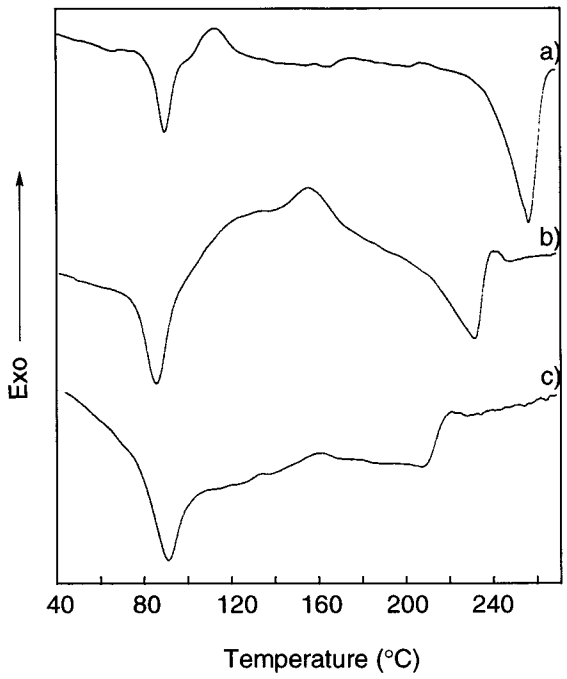

Figure 2. DSC charts of the as-prepared samples: (a) SPS, (b) SPS-*graft*-PIP-19.4, (c) SPS-*graft*-APS-17.3.

ence of one or several weak exothermic peaks is suspected. In each sample, of course, some phase transition should have occurred during the endothermic and the exothermic reactions. According to the reported melting temperature of SPS homopolymer,[31−34] the endothermic peaks in the 160−270 °C range correspond to the crystal melting. Attribution of the other peaks was studied by WAXD as below.

Figure 3 shows the WAXD diffractograms of as-prepared (namely the initial states of) SPS, SPS-*graft*-PIP-19.4, and SPS-*graft*-APS-17.3 at room temperature. All the patterns of as-prepared samples showed evident crystalline reflection peaks. These diffractograms were well explained by the unit cell of the δ-form. (For simplicity, we use the terminology for SPS homopolymer also for the graft copolymers.)

Next, each of as-prepared sample was heated in the sample stage of the WAXD instrument at the rate of 10 °C/min (the same heating rate as the DSC experiments) up to 130 °C and was held at the temperature for 1 h, and then the WAXD pattern at the temperature was recorded. We regard this WAXD pattern as giving information about the physical form after the endothermic reaction at 80−100 °C range. Figure 4 shows the WAXD diffractograms of as-prepared SPS, SPS-*graft*-PIP-19.4, and SPS-*graft*-APS-17.3 at 130 °C. Though the reflection peaks are broad, the diffractograms of SPS and SPS-*graft*-PIP-19.4 are explained by the γ form based on the peaks at $2\theta = 9°$ and 16°. On the other hand, the diffractogram of SPS-*graft*-APS-17.3 at this temperature was explained by the "helical" mesomorphic form based on two broad peaks at $2\theta =$ ca. 10° and 20°.

To clarify the physical forms before melting, each sample annealed at a temperature slightly below the onset of the melting endothermic peak was studied. As-prepared (fresh) samples were heated to a prefixed temperature and were held at the temperature for 1 h in the same way as above. Figure 5 shows the WAXD patterns of SPS, SPS-*graft*-PIP-19.4, and SPS-*graft*-APS-17.3 heated to, and taken at, 220, 210, and 170 °C, respectively. SPS is identified to be in the α' form based on the peak at $2\theta = 6.7°$, several peaks between $2\theta =$ 10° and 15°, and the absence of peaks between $2\theta =$ 15° and 19°. SPS-*graft*-PIP-19.4 showed the peaks at $2\theta = 6.2°$ (located at the slightly smaller angle side compared with the peak at $2\theta = 6.7°$ of the α form SPS in Figure 5a), 12.3°, 15.7°, and 18.5°, which peaks are explained by the β'' form. The physical form of SPS-*graft*-APS-17.3 at this temperature was, again, identified in terms of the "helical" mesomorphic form. However, a small amount of the γ form seems to be mixed.

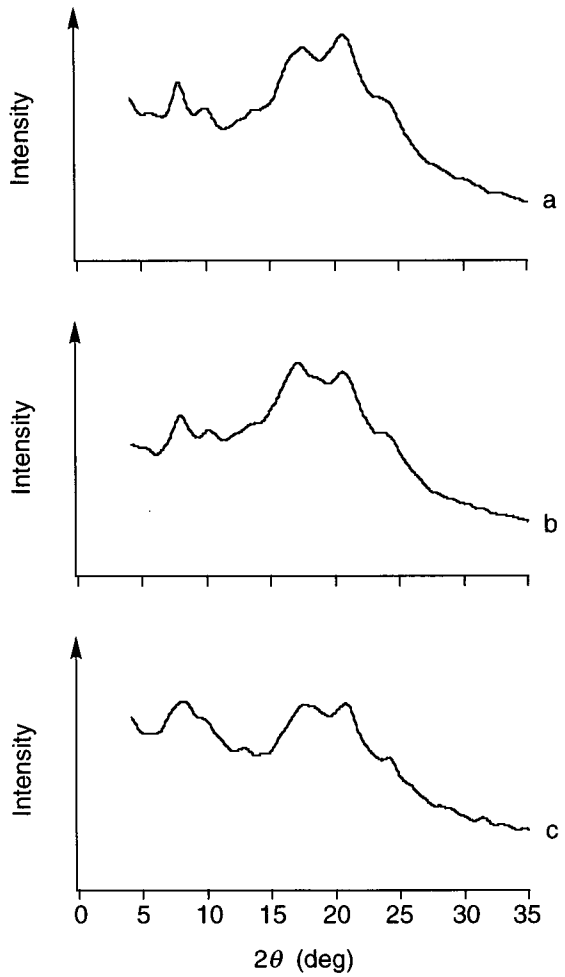

Figure 3. WAXD diffractograms of the as-prepared samples: (a) SPS, (b) SPS-*graft*-PIP-19.4, (c) SPS-*graft*-APS-17.3.

On the basis of above-mentioned WAXD studies, the transition schemes of physical forms of as-prepared samples on heating are summarized in Figure 6. As has been reported in former studies,[2−4] the δ form of SPS homopolymer transformed into the γ form through the first endothermic peak in the 80−100 °C range of the DSC charts, removing the solvent molecules (Figure 1a). At the higher temperature, the γ form of SPS transformed to the α' form and melted at ca. 250 °C. As-prepared SPS-*graft*-PIP-19.4 was in the δ form. This graft copolymer transformed into the γ form through the first endothermic peak at 80−100 °C range (Figure 1b), as is so in the case of the homopolymer. At the higher temperature, however, SPS-*graft*-PIP-19.4 transformed into the β'' form and melted at ca. 230 °C. As-prepared SPS-*graft*-APS-17.3 was also in the δ form. The endothermic peak of this copolymer in the 80−100 °C range (Figure 1c) may be due to the removal of the

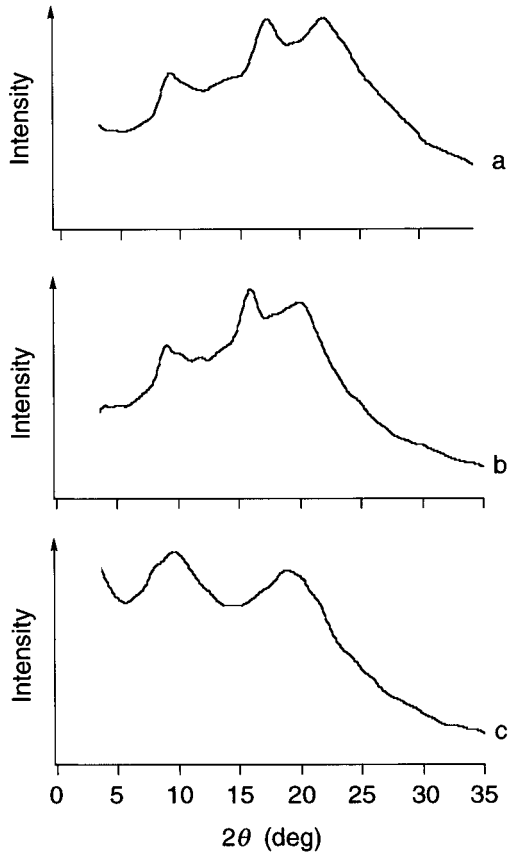

Figure 4. WAXD diffractograms of the samples heated to, and taken at, 130 °C after 1 h of holding: (a) SPS, (b) SPS-*graft*-PIP-19.4, (c) SPS-*graft*-APS-17.3.

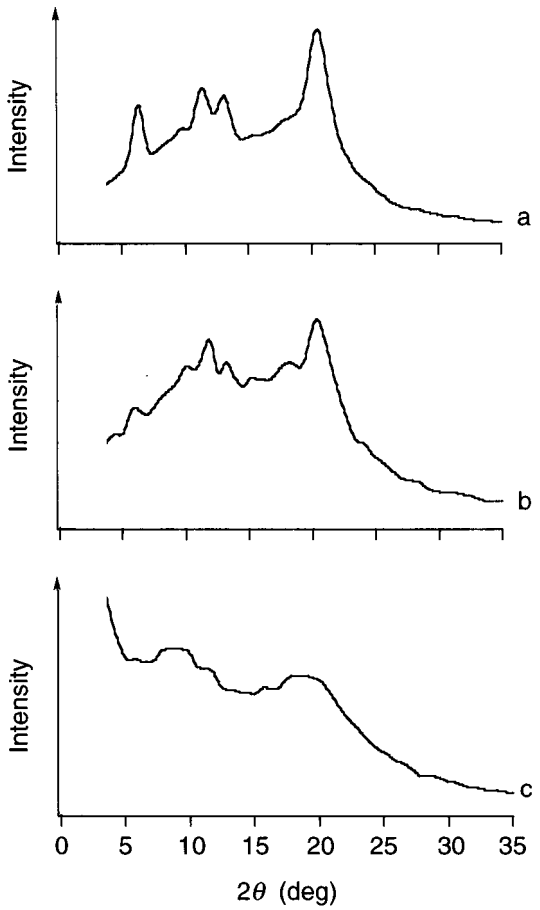

Figure 5. WAXD diffractograms of the samples heated to and taken at the prefixed temperatures after 1 h of holding: (a) SPS at 220 °C, (b) SPS-*graft*-PIP-19.4 at 210 °C, (c) SPS-*graft*-APS-17.3 at 170 °C.

solvent molecules and the rearrangement of molecular chains, as was so in the case of SPS or SPS-*graft*-PIP-19.4. Above this temperature range, SPS-*graft*-APS-17.3 was in the "helical" mesomorphic form, and at the higher temperature, the γ form may be mixed, showing the melting endothermic peak in the DSC scan.

We would like to compare above-mentioned results with the cases of syndiotactic random copolymers.[24,26] As for SPS after introduction of *p*-MS comonomeric units studied by Manfredi et al.,[24] as-prepared samples with small fractions (<7 mol %) of *p*-MS were in the δ form as in the case of pure SPS. However, another as-prepared sample containing 20 mol % of *p*-MS was in the γ form. By combining these results with their observation that SPS homopolymer can crystallize directly into the γ form by using of suitable solvents, they assumed that solvent molecules which are not suitable for the cavities of the δ form tend to favor the formation of the γ form. This assumption holds also for the results reported by Hong et al.[26] While as-prepared copolymers of SPS with isoprene comonomeric units were in the δ form, as-prepared copolymers of SPS with 2-vinylnaphthalene comonomeric units were in the γ form. The bulkiness of the latter comonomeric units may not allow the solvent molecules to be accommodated for the formation of the δ form, favoring the γ form. According to this point of view, one could have assumed that the syndiotactic graft copolymers with the long (bulky) side chains may favor the formation of the γ form. The formation of the δ form in the syndiotactic graft copolymers indicates that the side chains were sufficiently separated from each other on the main chain, and accordingly, the main chain had enough length of successive unbranched constituent to crystallize into the δ form.

Though the side chains may be separated from each other and the branches are coarsely distributed on the main chain, they did affect the polymorphic behaviors of the main chain of SPS, as are shown in Figure 6. This point will be discussed later together with the results of melt crystallization.

Thermal Behavior of Melt-Crystallized Samples. The samples subjected to the DSC experiments in the previous section were allowed to cool to room temperature in the DSC furnace and then scanned again. The samples should have been crystallized upon cooling from the melt. Before discussing the results of these second scans, we would like to clarify the physical forms of the samples cooled slowly from the melt. The as-prepared (fresh) samples were heated in the sample holder of the WAXD instrument at 10 °C/min up to ca. 300 °C, held at the temperature for 1 h, and allowed to cool to room temperature. Figure 7 shows the WAXD patterns of thus-prepared SPS, SPS-*graft*-PIP-19.4, and SPS-*graft*-APS-17.3. SPS was identified to be in the β' modification. The physical form of SPS-*graft*-PIP-19.4 is not clear, but the α and the β forms may coexist, according to the lowered intensity of the peak at $2\theta = 12.3°$ and the broadness of the peak at $2\theta =$ ca. 7°. On the other hand, only the diffuse scattering was observed for SPS-*graft*-APS-17.3. It should be noted that the diffractogram of the latter sample does not show the intensity maximum at $2\theta =$ ca. 10° (compare Figure 7c with

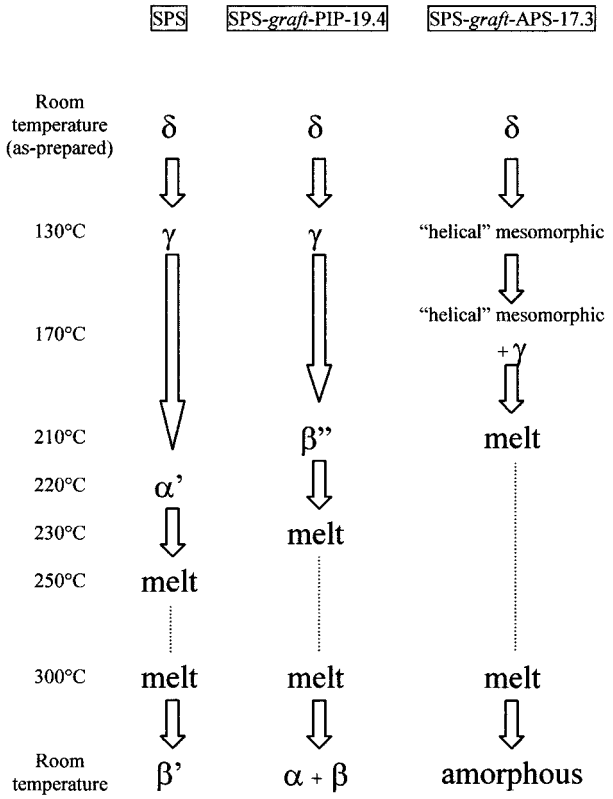

Figure 6. Transition schemes of the physical forms of as-prepared samples: (a) SPS (b) SPS-*graft*-PIP-19.4, (c) SPS-*graft*-APS-17.3.

Figure 4c), and accordingly, the sample was not in the mesomorphic form but in an amorphous state.[4] These results for the melt-crystallized samples are also shown in Figure 6.

Figure 8 shows the DSC charts of SPS, SPS-*graft*-PIP-9.2, SPS-*graft*-PIP-19.4, SPS-*graft*-APS-11.8, and SPS-*graft*-APS-17.3 during the second heating scan. (Though the graft chain contents were different, the length of PIP and APS side chains was fixed in each type of graft copolymer.) A distinct endothermic peak of crystal melting was observed for SPS. SPS-*graft*-PIP-9.2 showed an exothermic peak at ca. 155 °C and an endothermic peak of melting. The similar feature of the exothermic and the endothermic (melting) peaks was observed also for SPS-*graft*-PIP-19.4, though the peaks were shifted to the lower temperature side with the reduced peak area. The exothermic peaks may be attributed to development of the crystallinity (probably into the α form).[4]

In the case of SPS-*graft*-APS-11.8, the exothermic peak was not observed. Though the physical form is not identified due to the limited amount of this sample, at least, the sample was crystallized according to the existence of the endothermic peak of melting; the melting temperature was depressed, and the peak area was reduced, as well as SPS-*graft*-PIP-19.4.

As for SPS-*graft*-APS-17.3 (Figure 8e), the crystalline melting peak disappeared, as is expected from the result of WAXD (Figure 7c). Here we would like to focus on the crystallinity of this sample.[30] It must be remembered that the as-prepared state of this sample was the δ form, indicating that the main chain has enough length of successive unbranched constituent to allow crystallization. Why the sample that was cooled from the melt was in the amorphous state? One explanation is a slow

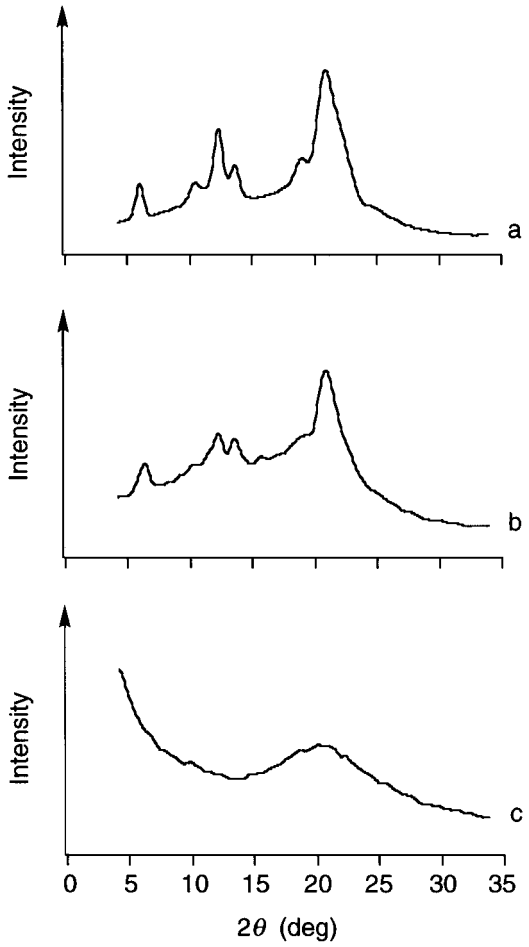

Figure 7. WAXD diffractograms of the samples after slow cooling from the melt: (a) SPS, (b) SPS-*graft*-PIP-19.4, (c) SPS-*graft*-APS-17.3.

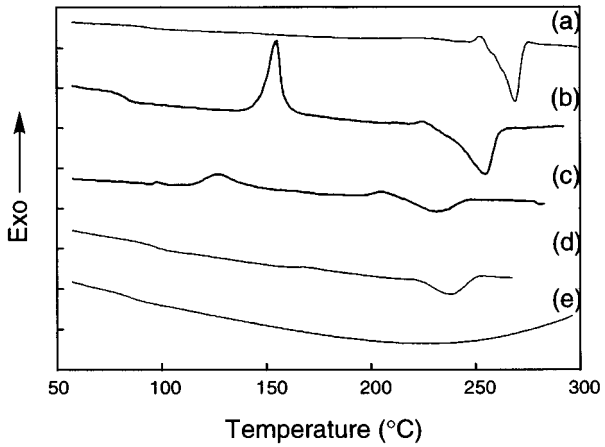

Figure 8. DSC charts of the samples after slow cooling from the melt: (a) SPS, (b) SPS-*graft*-PIP-9.2, (c) SPS-*graft*-PIP-19.4, (d) SPS-*graft*-APS-11.8, (e) SPS-*graft*-APS-17.3.

crystallization rate of the graft copolymer, and the other is loss of crystallinity itself. We examined, therefore, another run for SPS-*graft*-APS-17.3 by DSC, which was cooled much more slowly (at 1.0 °C/min) from the melt. Even in this case, the melting peak did not appear in the heating scan of DSC chart. Accordingly, we assumed that the crystallinity of SPS (from the melt) was lost by introducing ca. 17 wt % of APS side chains.

For comparison, blends of SPS with APS (SPS-*blend*-APS)[22−24] were tentatively prepared. The samples were

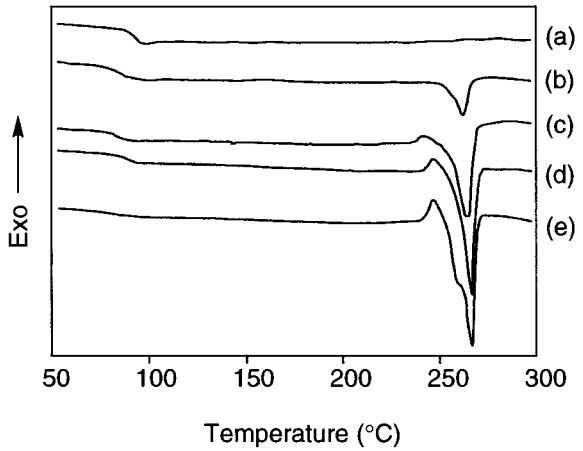

Figure 9. DSC charts of the blends of SPS with APS after slow cooling from the melt: (a) SPS-*blend*-APS-100, (b) SPS-*blend*-APS-78, (c) SPS-*blend*-APS-50, (d) SPS-*blend*-APS-21, (e) SPS-*blend*-APS-0.

once melted in the DSC furnace and then cooled slowly to room temperature. The heating scans of thus-prepared (melt-crystallized) samples are shown in Figure 9. The melting temperature decreased only slightly with increasing APS fraction. It should be noted that even when 78 wt % of APS is blended, a distinct crystal melting peak is observed. These results indicate that, compared to blending, grafting APS onto SPS main chain has an extremely strong influence on the crystallization of SPS constituent.

Even when the result for SPS-*graft*-APS-17.3 is compared with the random copolymer of SPS with 20 mol % of *p*-MS comonomeric units,[25] the influence of the grafted APS side chains appears to be very strong. The former (graft copolymer) could not crystallize from the melt, while the latter (random copolymer) has been reported to crystallize into the α form; the two samples have a comparable amount of heterogeneity. In this case, one would rather expect higher crystallinity for the graft copolymer, because the graft copolymer should have a longer average length of successive SPS (unbranched) constituents than the random copolymer, when the same amount of heterogeneities is introduced. The reason for this discrepancy between the expectation and the experimental result will be discussed after morphological evidence is presented in the next section.

AFM Observation of Melt-Crystallized Samples. Melt-crystallized samples for AFM were differently prepared as follows. Each of the as-prepared samples on a glass slide was melted on a hot plate to form a thin layer and cooled to room temperature. Then a drop of fuming nitric acid (98%) was put on the sample and was held for 6 h at room temperature in order to remove the surface and to expose the internal structure. Finally, the samples were washed with distilled water and dried.

Figure 10 shows AFM images of (a) SPS-*graft*-PIP-9.2 and (b) SPS-*graft*-PIP-19.4. In the case of SPS homopolymer and SPS-*graft*-APS, only fractured textures without special feature were observed, and accordingly, AFM images of them are not presented here. On the other hand, in the case of SPS-*graft*-PIP-9.2, granular protrusions were observed in addition to the cross section of stacked lamellae. In another AFM image which is not shown here, a sperulitic texture was also observed. In the case of SPS-*graft*-PIP-19.4, protrusions of higher density were observed; the other features on

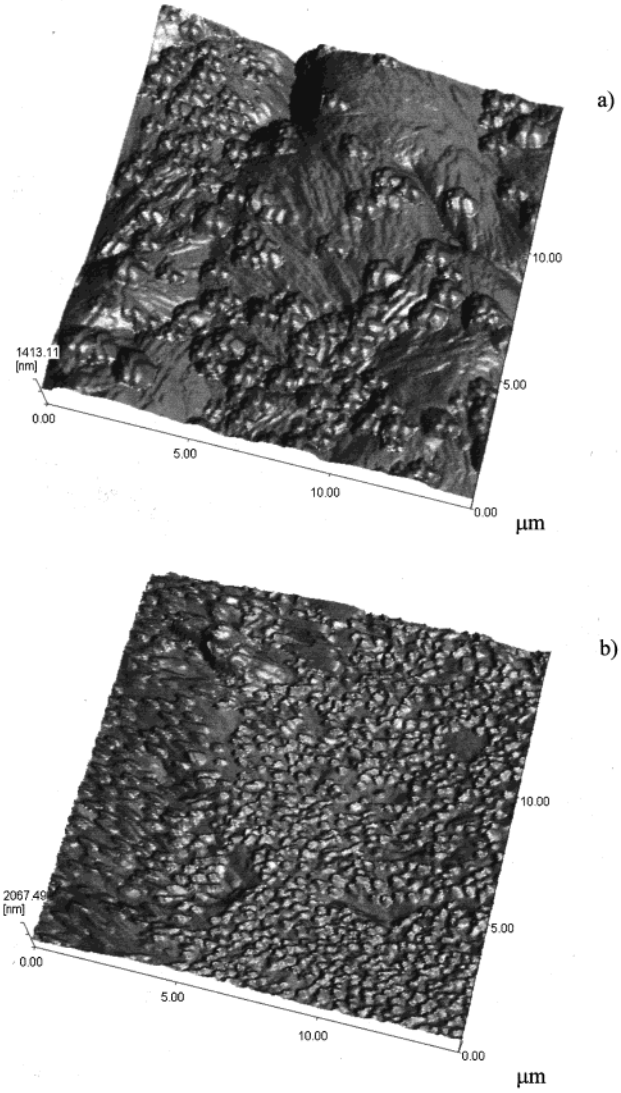

Figure 10. AFM images of (a) SPS-*graft*-PIP-9.2 and (b) SPS-*graft*-PIP-19.4 after the treatment by fuming nitric acid.

the surface were covered by the protrusions. Whatever the protrusions were, they must be related to the PIP graft chains, because the density of protrusions increased with an increase in the fraction of the PIP graft chain. It should be noted that the size of each protrusion was almost maintained though the density was increased. There may be some restriction for the transportation of the PIP segments; that is, the PIP segments may be connected to the main chain even after the heating to 300 °C.

Effect of the Graft Chains on Crystallization. It is a self-evident truth that crystallization of a polymer from the melt requires conformational (intramolecular) and crystalline (intermolecular) ordering. Intramolecular ordering may be inhibited by configurational irregularity (poor stereoregularity) or by introduction of heterogeneity into the molecule through copolymerization. In the cases of syndiotactic graft copolymers studied in this paper, they should have the ability of intramolecular ordering because the as-prepared samples were in the δ form crystallites. On the other hand, intermolecular ordering will not occur if cohesive power of the molecular segment is not enough to overcome, e.g., the friction force for reptation of the chain. It should be noted that the cohesive power originates not only from

attractive forces but also from repulsive forces in a multicomponent system.

In the case of SPS-*graft*-PIP, constituents of the main chain (SPS) and the side chains (PIP) are immiscible, and accordingly, these segments tend to separate from each other, as is known from Figure 10. Then the immiscibility may contribute to the cohesive power for the crystallization of the SPS constituents, compensating for the increased friction force for reptation by the introduction of the side chains. We think, therefore, that the intermolecular ordering was possible and the crystallinity of SPS-*graft*-PIP was maintained, though the polymorphic behavior was different from the homopolymer.

On the other hand, in the case of SPS-*graft*-APS, constituents of the main chain and the side chains (APS) are miscible. The cohesive power of the SPS constituent may not be so different from that of the homopolymer, while the molecular friction force may have been increased by the side chains. Therefore, the intermolecular ordering of SPS-*graft*-APS may be relatively disadvantageous. Once the intermolecular order of the as-prepared sample (in the δ form) was reduced by removing the guest (solvent) molecules, reordering to form the γ form should be very difficult. This may be the reason why the sample heated above 130 °C was mostly in the mesomorphic form, only having the intramolecular order. Furthermore, the crystallinity from the melt was greatly reduced, and totally lost in the case of SPS-*graft*-APS 17.3, probably because of the reduced ability of intermolecular ordering.

Conclusion

The polymorphic behaviors of syndiotactic graft copolymers were investigated, mainly by DSC and WAXD. As-prepared SPS-*graft*-PIP-19.4 was in the δ form. This graft copolymer transformed into the γ form on heating to 130 °C and into the β'' form on heating to 210 °C. Finally the sample was melted at ca. 230 °C. In the melt-crystallized SPS-*graft*-PIP-19.4, the α and the β forms were thought to coexist. As-prepared SPS-*graft*-APS-17.3 was also in the δ form. By heating to 130 °C, SPS-*graft*-APS-17.3 turned into the "helical" mesomorphic form, and at the higher temperature, coexistence of the γ form was detected along with the mesomorphic form. Though SPS-*graft*-APS-11.8 could crystallize from the melt, SPS-*graft*-APS-17.3 cooled from the melt was in an amorphous state. The effect of the graft chains on crystallinity was discussed in terms of the friction force for reptation and the cohesive power.

Acknowledgment. This work has been supported in part by the Venture Business Laboratory (VBL) in Kyoto University.

References and Notes

(1) Ishihara, N.; Seimiya, T.; Kuramoto, M.; Uoi, M. *Macromolecules* **1986**, *19*, 2464.
(2) Chatani, Y.; Shimane, Y.; Inoue, Y.; Inagaki, T.; Ishioka, T.; Ijitsu, T.; Yukinari, T. *Polymer* **1992**, *33*, 488.
(3) Guerra, G.; Vitagliano, V. M.; De Rosa, C.; Petraccone, V.; Corradini, P. *Macromolecules* **1990**, *23*, 1539.
(4) Manfredi, C.; De Rosa, C.; Guerra, G.; Rapacciuolo, M.; Auriemma, F.; Corradini, P. *Macromol. Chem. Phys.* **1995**, *196*, 2795.
(5) Pradère, P.; Thomas, E. L. *Macromolecules* **1990**, *23*, 4954.
(6) De Rosa, C. *Macromolecules* **1996**, *29*, 8460.
(7) De Rosa, C.; Rapacciuolo, G.; Guerra, G.; Petraccone, V.; Corradini, P. *Polymer* **1992**, *33*, 1423.
(8) Chatani, Y.; Shimane, Y.; Ijitsu, T.; Yukinari, T. *Polymer* **1993**, *34*, 1625.
(9) Tsuji, M.; Okihara, T.; Tosaka, M.; Kawaguchi, A.; Katayama, K. *MSA Bull.* **1993**, *23*, 57.
(10) Tosaka, M.; Hamada, N.; Tsuji, M.; Kohjiya, S.; Ogawa, T.; Isoda, S.; Kobayashi, T. *Macromolecules* **1997**, *30*, 4132.
(11) Hamada, N.; Tosaka, M.; Tsuji, M.; Kohjiya, S.; Katayama, K. *Macromolecules* **1997**, *30*, 6888.
(12) Tosaka, M.; Hamada, N.; Tsuji, M.; Kohjiya, S. *Macromolecules* **1997**, *30*, 6592.
(13) Tosaka, M.; Tsuji, M.; Kohjiya, S.; Cartier, L.; Lotz, B. *Macromolecules* **1999**, *32*, 4905.
(14) Chatani, Y.; Shimane, Y.; Inagaki, T.; Ijitsu, T.; Yukinari, T.; Shikuma, H. *Polymer* **1993**, *34*, 1620.
(15) De Rosa, C.; Guerra, G.; Petraccone, V.; Pirozzi, B. *Macromolecules* **1997**, *30*, 4147.
(16) Endo, K.; Senoo, K. *Macromol. Rapid Commun.* **1998**, *19*, 563.
(17) Endo, K.; Senoo, K. *Polym. J.* **1999**, *31*, 817.
(18) Endo, K.; Senoo, K. *Polymer* **1999**, *40*, 5977.
(19) Endo, K.; Senoo, K. *Polym. Bull.* **2000**, *44*, 25.
(20) Gedde, U. W. In *Polymer Physics*; Chapman & Hall: London, 1995; Chapter 7, p 131.
(21) Ermer, H.; Thomann, R.; Kressler, J.; Brenn, R.; Wünsch, J. *Macromol. Chem. Phys.* **1997**, *198*, 3639.
(22) Hong, B.; Jo, W.; Kim, J. *Polymer* **1998**, *39*, 3753.
(23) Woo, E. M.; Wu, F. S. *J. Polym. Sci., Part B: Polym. Phys.* **1998**, *36*, 2725.
(24) Manfredi, C.; Guerra, G.; De Rosa, C.; Busico, V.; Corradini, P. *Macromolecules* **1995**, *28*, 6508.
(25) Thomann, R.; Sernetz, F. G.; Heinemann, J.; Steinmann, S.; Mühaupt, R.; Kressler, J. *Macromolecules* **1997**, *30*, 8401.
(26) Hong, B.; Kim, K.; Cho, J.; Jo, W. *Macromolecules* **1998**, *31*, 9081.
(27) Guerra, G.; De Rosa, C.; Vitagliano, V. M.; Petraccone, V.; Corradini, P.; Karasz, F. E. *Polym. Commun.* **1991**, *32*, 30.
(28) Guerra, G.; De Rosa, C.; Vitagliano, V. M.; Petraccone, V.; Corradini, P. *J. Polym. Sci., Part B: Polym. Phys.* **1991**, *29*, 265.
(29) Senoo, K.; Endo, K.; Murakami, S.; Tosaka, M. *Chem. Lett.* **2000**, *3*, 278.
(30) Murakami, S.; Tanno, K.; Tsuji, M.; Kohjiya, S. *Bull. Inst. Chem. Res., Kyoto Univ.* **1995**, *72*, 418.
(31) Arnauts, J.; Berghmans, H. *Polym. Commun.* **1990**, *31*, 343.
(32) Gvozdic, N. V.; Meier, D. J. *Polym. Commun.* **1991**, *32*, 183.
(33) Gvozdic, N. V.; Meier, D. J. *Polym. Commun.* **1991**, *32*, 493.
(34) Lin, R. H.; Woo, E. M. *Polymer* **2000**, *41*, 121.

MA001238A